

Cationic surfactant-triggered formation of a supramolecular hydrogel by a negatively charged L-valine derivative†

Masahiro Suzuki,^a Teruaki Sato,^b Hirofusa Shirai^b and Kenji Hanabusa^a

Received (in Montpellier, France) 30th August 2006, Accepted 13th October 2006

First published as an Advance Article on the web 7th November 2006

DOI: 10.1039/b612478j

Octadecylaminocarbonyl-L-valyl-N-suberic acid sodium salt (**1**), prepared from octadecylaminocarbonyl-L-valine, has been found to function as a cationic surfactant-triggered hydrogelator. Although **1** was water-soluble and had no hydrogelation ability, it formed a hydrogel in the presence of a cationic surfactant. Hydrogelation at room temperature occurred by addition of a cationic surfactant solution to an aqueous solution of **1**. FT-IR studies demonstrated that the driving forces for hydrogelation were non-covalent intermolecular interactions such as hydrophobic and hydrogen bonding interactions. In addition, fluorescence spectroscopy using 8-anilino-1-naphthalenesulfonic acid sodium salt (ANS) as a probe demonstrates that some aggregates such as micelles play an important role in the self-assembly of **1** into nanofibers. Moreover, it was found that the combination of **1** and dodecyl(trimethyl)ammonium chloride (DTMACl) provided a suitable hydrophobic–hydrophilic balance, and formed a thermally stable hydrogel.

Introduction

Low-molecular-weight gelators have attracted much attention not only because of their academic interest but also their potentially wide applications to industrial fields such as cosmetics, foods, medical science, and tissue engineering.^{1–12} Such gelators, which are small molecules, form various supramolecular polymers through hydrogen bonding, van der Waals (hydrophobic), and π -stacking interactions, and create a three-dimensional network, leading to the formation of supramolecular gels. Of particular interest for materials science is smart gels; *i.e.*, the gelation properties of gels controlled by external stimuli such as heat, light, magnetic or electric fields, pH, sound, and chemical reactions.^{13–22} Such responsive systems are highly desirable in applications such as drug delivery, catalysis and nanoscopic assemblies with interesting optical and electrical properties.^{23,24} A promising approach towards the smart gels is the introduction of functional groups responsive to external stimuli; *e.g.*, photochromic or photoreactive groups for light and the carboxyl group for pH.

It is very important for the development of good gelators that they are simply and effectively synthesized and environmentally friendly materials. L-Amino acid-based gelators are one of the best gelators according to the concepts; L-amino acids are safe for the environment and living organisms and cheap, and the synthetic methodologies for the synthesis of

many amino acid-based compounds are already established (simple synthetic procedure). Recently, we have reported all-powerful organogelators based on L-valine and L-isoleucine derivatives that can form organogels in many organic solvents and oils.²⁵ The water-soluble L-valine and L-isoleucine derivatives with a sodium carboxylate group showed no hydrogelation ability in addition to a low organogelation ability. Very interestingly, we have found that a hydrogel is formed by addition of a cationic surfactant. In this paper, we describe cationic surfactant-triggered hydrogel formation using the L-valine derivative. As cationic surfactants, dodecyl(trimethyl) ammonium chloride (DTMACl, cmc = 20 mM), hexadecyl (trimethyl)ammonium chloride (HDTMACl, cmc = 1.3 mM) and bis(dodecyl)(dimethyl)ammonium bromide (DDMABr, cmc = 0.17 mM) were used²⁶ (Fig. 1).

Results and discussion

As reported previously,²⁵ compound **1** functioned as a water-soluble organogelator for some organic solvents and oils including alcohols, DMF, DMSO, salad oil, linseed oil, paraffin, triolein, kerosene, and propylene carbonate, but not for water. In the presence of cationic surfactants, **1** formed a hydrogel. The hydrogelation properties were evaluated by two

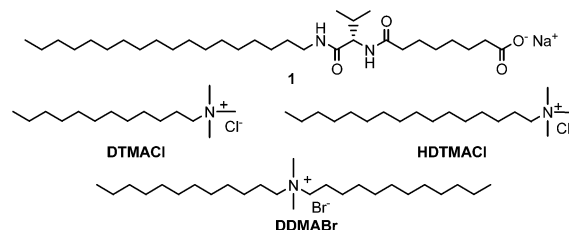


Fig. 1 Chemical structures of L-valine derivative and cationic surfactants.

^a Graduate School of Science and Technology, Shinshu University, Ueda, Nagano 386-8567, Japan. E-mail: msuzuki@giptc.shinshu-u.ac.jp; Fax: +81 268 21 5608; Tel: +81 268 21 5415

^b Department of Functional Polymer Science, Faculty of Textile Science and Technology, Shinshu University, Ueda, Nagano 386-8567, Japan

† Electronic supplementary information (ESI) available: Table for minimum gel concentration and FE-SEM image of the dried sample prepared from an aqueous solution of dodecyl(trimethyl)ammonium chloride (DTMACl). See DOI: 10.1039/b612478j

Table 1 Hydrogelation properties of **1** at 25 °C^a

Surfactant- 1 /mol	[Surfactant]/mM	DTMACl		HDTMACl		DDMABr	
		Method 1	Method 2	Method 1	Method 2	Method 1	Method 2
0 : 1	0	—	—	—	—	—	—
0.2 : 1	3.64	VS	GTL	VS	GTL	GT	GTL
0.3 : 1	5.46	VS	GTL	GT	GTL	GT	GTL
0.4 : 1	7.28	GT	GTL	GTL	GTL	GTL	GTL
0.6 : 1	10.92	GTL	GO	GTL	GO	GO → P ^b	P
0.8 : 1	14.56	P	P	GTL	GO	GO → P ^b	P
1.0 : 1	18.27	P	P	P	P	GO → P ^b	P
1.2 : 1	21.84	GTL	GTL	GTL	GTL	GO → P ^b	P
1.4 : 1	25.48	GTL	GTL	GTL	GTL	GO → P ^b	P
1.6 : 1	29.12	GTL	GTL	GTL	GTL	GO → P ^b	P
1.8 : 1	32.75	GO → P ^b	P	GTL	GTL	—	—
2.0 : 1	36.40	GO → P ^b	P	GTL	GTL	—	—

^a [**1**] = 18.3 mM and surfactant : **1** is the ratio of surfactant and gelator. ^b The hydrogels were unstable and they changed to precipitates within 1 month. GTL: translucent gel. GT: transparent gel. GO: opaque gel. VS: viscous solution. P: precipitate. —: no hydrogelation.

procedures; one is the dissolution of gelators in an aqueous solution of a surfactant (method 1), the other is the mixing of aqueous solutions of gelators and surfactant at 25 °C (method 2).

Hydrogelation properties

Using method 1, the hydrogelation properties of **1** were examined and listed in Table 1. **1** had no hydrogelation abilities, however, it formed a hydrogel in the presence of a cationic surfactant and the hydrogelation properties significantly depended on the concentration of the surfactants. For DTMACl, when the ratio of surfactant and gelator (DTMACl-**1**) was 0.4 : 1, **1** formed a transparent gel. The transparent hydrogels were formed at 0.3 : 1 for HDTMACl-**1** and 0.2 : 1 for DDMABr-**1**. It is noteworthy that **1** forms a hydrogel by addition of a lower concentration of surfactant with increasing hydrophobicity of the surfactant. For DTMACl and HDTMACl, **1** lost its hydrogelation ability around surfactant : **1** = 1.0 : 1 and a white solid precipitated. Strangely, the precipitate never dissolved in water even when the solution was heated around its boiling point for 10 min. The elemental analysis and ¹H-NMR measurements indicate that the white precipitate is a complex consisting of **1** and surfactant, formed by the ionic exchange between Na⁺ and (surfactant)⁺. At surfactant : gelator > 1.0 : 1, excess surfactants solubilize the complex of **1** and the surfactant. In addition, the hydrogels formed above DTMACl-**1** = 1.8 : 1 and DDMABr-**1** = 0.6 : 1 were unstable and they changed to precipitates within 1 month. Such hydrogelation behavior never takes place in the presence of anionic or non-ionic surfactants (sodium dodecylsulfate, Tritons, and Tweens) as well as inorganic salts (NaCl and KCl). Therefore, the ion exchange from Na⁺ to (surfactant)⁺ plays a role in the hydrogelation.

From the results of method 1, we investigated hydrogelation at room temperature using method 2. When an aqueous solution of a surfactant was added to an aqueous solution of **1** with vigorous stirring, a hydrogel was formed within 30 s. For HDTMACl, the hydrogelation properties hardly depended on the methods of hydrogelation, while a different

result was obtained at high DTMACl-**1** (≥ 1.8 : 1) and DDMABr-**1** (≥ 0.6 : 1) ratios; **1** precipitated by addition of DTMACl or DDMABr. It is well-known that a surfactant has a critical micelle concentration (cmc). Because the concentrations of HDTMACl and DDMABr are above the cmc under the experimental conditions of hydrogelation, they form a cationic micelle. Below the cmc, however, no hydrogel formation was observed in these systems. Therefore, the electrostatic interaction between L-valine derivatives and cationic micelles is an important role in hydrogelation. In contrast, DTMACl-**1** forms a hydrogel below and above the cmc of DTMACl. Above the cmc, the hydrogelation proceeds by the same mechanism as other surfactants, while the formation of a hydrogel may occur through ionic exchange.

Furthermore, we examined the formation of hydrogels using a common aliphatic acid sodium salt such as lauric acid and palmitic acid, as well as an amide acid such as sodium 6-(N-lauroylamino)hexanoate. However, a hydrogel was never formed. This fact indicates that the L-valine segment plays an important role in the formation of the hydrogel. It is likely that the amide group and the chiral isopropyl group in L-valine are important for self-assembly into nanofibers. In addition, this system should be classified as a two-component gelation system.^{27,28}

TEM and FE-SEM

It is well-known that a gelator molecule constructs nano-scaled superstructures such as nanofibers, nanoribbons and nanoparticles in a supramolecular hydrogel.^{4,5} Fig. 2 shows the TEM and FE-SEM images of the superstructures built up with **1** in aqueous solution (A, D), transparent hydrogel (DTMACl-gelator = 0.4 : 1; B, E) and opaque hydrogel (DTMACl : gelator = 2.0 : 1; C, F). The TEM image of a dried sample from an aqueous solution of **1** demonstrated that **1** formed some short nanofibers, 30–50 nm in diameter and 200–400 nm in length (D), and some sheet and fiber structures, 300–600 nm in width, were observed in the SEM image (A). **1** has no hydrogelation ability because of the formation of a small nanostructure. On the other hand, DTMACl-**1** created a three-dimensional network by self-assembly of nanofibers

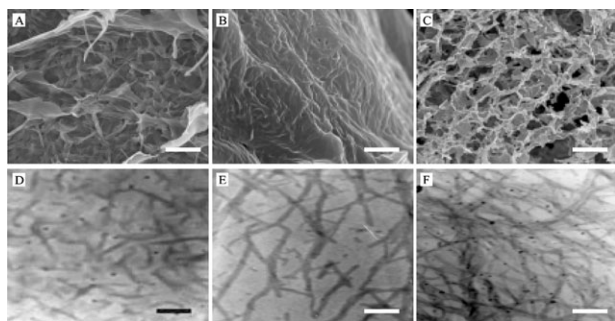


Fig. 2 FE-SEM (A–C) and TEM (D–F) images of the superstructures built up by **1** in aqueous solution (A, D), transparent hydrogel (DTMACI–**1** = 0.4 : 1; B, E) and opaque hydrogel (DTMACI–**1** = 2.0 : 1; C, F). Scale bars are 200 nm.

having a diameter of several tens of nanometers and more than 1 μm in length, which indicated that the nanofiber becomes long and entangles upon addition of DTMACI. Similar images were observed for other surfactant systems. In addition, the SEM image of the dried sample prepared by freeze drying of the surfactant solution under the same concentration showed no fibrous structure (see ESI†), indicating that the nanofibers shown in Fig. 2 are not worm-like micelle formed by the surfactant.

FT-IR study

In order to evaluate the driving forces for hydrogelation, we measured the FT-IR spectra. In CHCl_3 solution, the typical IR bands, arising from non-hydrogen bonded amide groups, were observed at 1655 cm^{-1} (amide I) and 1510 cm^{-1} (amide II). On the other hand, the IR spectrum showed the absorption bands at 1627 cm^{-1} (amide I) and 1560 cm^{-1} (amide II) in D_2O gel based on DTMACI–**1** (0.4 : 1), characteristic of the intermolecular hydrogen bonded amide groups. Furthermore, the absorption bands of antisymmetric ($\nu_{\text{as}}\text{C-H}$) and symmetric ($\nu_{\text{s}}\text{C-H}$) stretching vibrations in the alkyl chain appeared at low wavelengths, 2919 cm^{-1} and 2851 cm^{-1} , compared with those of **1** in CHCl_3 solution ($\nu_{\text{as}}\text{C-H} = 2929\text{ cm}^{-1}$ and $\nu_{\text{s}}\text{C-H} = 2856\text{ cm}^{-1}$). Such IR shifts imply the presence of a strong hydrophobic interaction in the D_2O gel.^{29,30} Therefore, the driving forces for the formation of a hydrogel are mainly hydrophobic interaction and complementary hydrogen bonding.

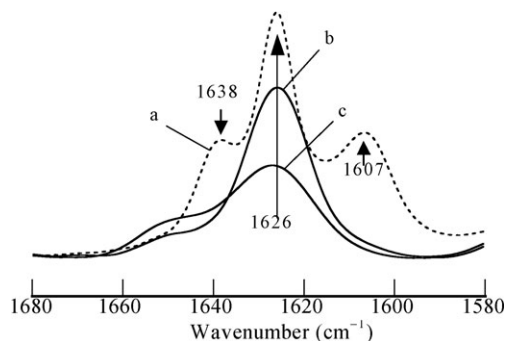


Fig. 3 FT-IR spectra of **1** and DTMACI–**1** (0.4 : 1) in D_2O . a: solution of **1**; b: gel of DTMACI–**1** ($25\text{ }^\circ\text{C}$); c: solution of DTMACI–**1** ($70\text{ }^\circ\text{C}$).

Fig. 3 shows the FT-IR spectra of D_2O solutions of **1** and DTMACI–**1** (0.4 : 1, $70\text{ }^\circ\text{C}$) and D_2O gels of DTMACI–**1** (0.4 : 1, $25\text{ }^\circ\text{C}$). In D_2O , **1** showed a total of three IR peaks at 1638 cm^{-1} and 1607 cm^{-1} in addition to 1626 cm^{-1} in the amide I region. In addition, the absorption bands of $\nu_{\text{as}}\text{C-H}$ and $\nu_{\text{s}}\text{C-H}$ were observed at 2919 cm^{-1} and 2851 cm^{-1} . These results indicate that **1** forms small nanoscale aggregates (as shown in Fig. 2) through hydrophobic interaction and hydrogen bonding with at least three binding modes (Scheme 1). In water, **1** first forms pre-aggregates through hydrophobic interactions and medium strength hydrogen bonding (1626 cm^{-1}), and then these aggregates grow into a lamella-like nanostructure with alternating direction through strong and weak hydrogen bonding corresponding to the IR peaks at 1607 cm^{-1} and 1638 cm^{-1} . The weak hydrogen bonding is relatively unstable because of steric hindrance between the isopropyl groups, and this may inhibit growth into a long nanofiber. On the other hand, the IR spectrum of the D_2O gel based on DTMACI–**1** ($25\text{ }^\circ\text{C}$) showed one absorption band at 1626 cm^{-1} arising from the hydrogen bonded amide I. At $70\text{ }^\circ\text{C}$, the gel changed to the solution state and the IR peak decreased, and a higher wavenumber shift of the IR peaks of the alkyl chains was observed. Moreover, the IR band, characteristic of free amide I, appeared around 1650 cm^{-1} in the solution state. This is attributed to the fact that the intermolecular hydrogen bonding and hydrophobic interactions are broken upon heating; consequently, a gel-to-sol transition takes place. It is interesting that the IR spectrum of the hydrogel is quite different from that of **1** in D_2O . This indicates that the nanostructure formed by **1** is different from that of DTMACI–**1** at the molecular level.

Fluorescence study

To elucidate the self-assembly process, the fluorescence spectra were measured using 8-anilino-1-naphthalenesulfonic acid sodium salt (ANS) as a probe. ANS is one of the more popular fluorescent probes for a hydrophobic environment.^{31,32} Fig. 4

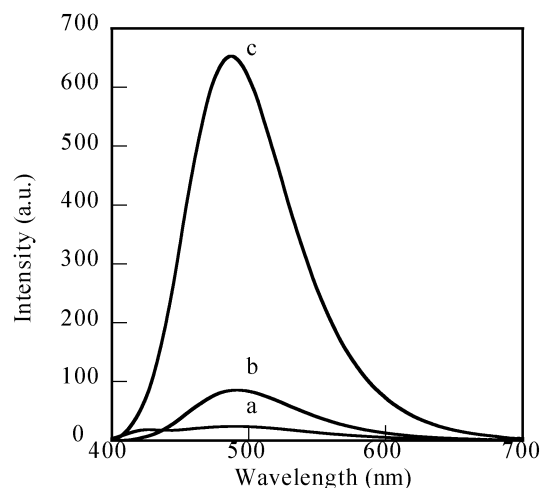


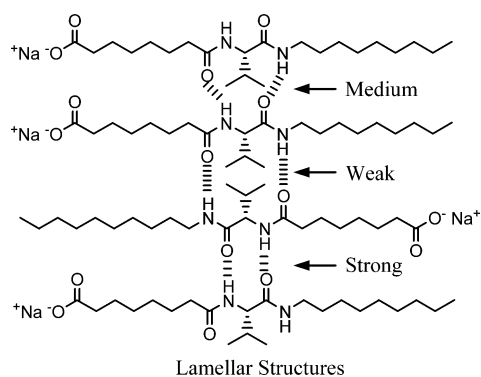
Fig. 4 Fluorescence spectra of ANS ($2.0 \times 10^{-5}\text{ M}$) in aqueous solutions of **1** (a) and DTMACI (b) and hydrogel based on DTMACI–**1** (0.4 : 1) (c). $[\text{1}] = 18.3\text{ mM}$, $[\text{DTMACI}] = 7.28\text{ mM}$. Excitation is 356 nm .

Table 2 Thermodynamic parameters for sol–gel transition of hydrogels and physical data

	$\Delta H_{\text{gel}}/\text{kJ mol}^{-1}$	MGC ^a /mM	Gel strength/kPa
DTMACI-1 (0.4 : 1)	52.6	3.7	1.91
HDTMACI-1 (0.4 : 1)	44.3	7.3	1.53
DDMABr-1 (0.4 : 1)	43.3	7.3	1.42

^a Minimum gel concentration.

shows the fluorescence spectra of ANS in aqueous solutions containing **1** (18.3 mM), DTMACI (7.28 mM), and DTMACI-1 (0.4 : 1). ANS showed a very small emission at 492 nm ($I = 18.2$) in an aqueous solution of **1**, and a blue shift in the maximum wavelength and an increase in the fluorescence intensity were observed compared with the emission in H₂O ($\lambda_{\text{max}} = 520$ nm, $I = 3.5$). In the aqueous solution of DTMACI (7.28 mM), the emission of ANS was observed at 491 nm ($I = 85.4$). The results indicate that **1** and DTMACI form some aggregates in water with a hydrophobic field and the emission is caused by the hydrophobic interaction between ANS and the aggregates. Because the aggregates formed by **1** have a negative charge, the interaction with ANS should be weak, leading to a small emission. In contrast, a large emission of ANS was observed at 486 nm ($I = 653$) in the DTMACI-1 hydrogel. As a control experiment, the fluorescence spectrum of ANS was measured in an aqueous solution of DTMACI under the conditions above the cmc (30 mM), resulting in an emission at 490 nm ($I = 350$). It is clear that the hydrophobicity in the field formed by DTMACI-1 is larger than that formed by DTMACI, and ANS molecules are incorporated into the hydrophobic field in nanofibers formed by DTMACI-1. As mentioned above, the ANS molecules have a weak interaction with the nanofibers of **1** because of an electrostatic repulsion. It is generally known that the incorporation of a charged fluorescent probe such as ANS into a hydrophobic field occurs through an electrostatic attraction in addition to a hydrophobic interaction. Indeed, ANS is hardly incorporated into the hydrophobic field of negatively charged micelle formed by sodium dodecylsulfate (SDS). Therefore, some aggregates formed by DTMACI like a micelle play an important role in not only the self-assembly of **1** into nanofibers but also the incorporation of ANS molecules into nanofibers.

**Scheme 1** Hydrogen bonding modes of **1** in H₂O.

Aggregation modes and hydrogelation mechanism

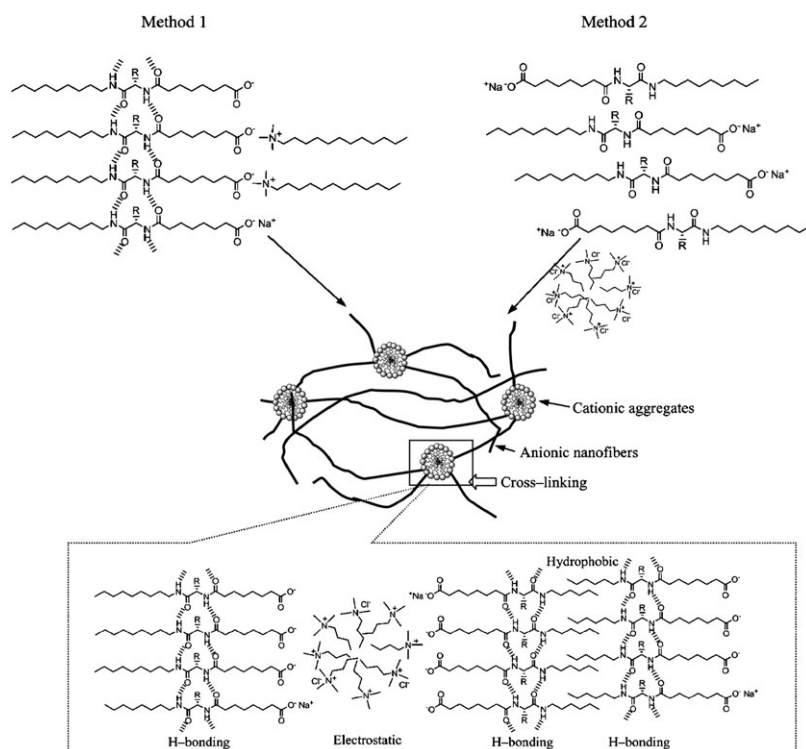
The results from the FT-IR and luminescence studies let us propose a mechanism for the cationic surfactant-triggered hydrogelation and aggregation modes of **1** as illustrated in Scheme 2. In method 1, after **1** is dissolved in a cationic surfactant solution by heating, the ion exchange reaction between Na⁺ and S⁺ takes place, which induces the self-assembly of **1** into the long nanofibers through only a medium strength hydrogen bonding mode (arising from the IR peak at 1626 cm⁻¹) in addition to hydrophobic interactions, being supported by the IR results. The cationic surfactant segments are aggregated into the micelle structure. In method 2, the small nanoaggregates of **1** electrostatically interact with a cationic micelle aggregate formed by a cationic surfactant and self-organizes into long nanofibers. The electrostatic interaction between the aggregates formed by **1** and those by the cationic surfactant may induce self-assembly into nanofibers, and a three dimensional network is created by cross-linking anionic nanofibers by cationic aggregates, which leads to the formation of a hydrogel.

Gel strength and thermal stability

Gel strength is one of the important factors in the application of hydrogels. The gel strengths of hydrogels based on **1** and surfactants (0.4 : 1) are listed in Table 2. Amongst the three systems, the hydrogel of DTMACI-1 showed the largest gel strength and the value was 1.91 kPa. It is likely that the gel strength is connected to the rigidity of self-assembled nanofibers; namely, the gel strength of a hydrogel having a three dimensional network formed by rigid nanofibers is large.³³ Probably, the combination of **1** and DTMACI provides a suitable hydrophilic–hydrophobic balance, which leads to the formation of relatively rigid nanofibers.

Fig. 5 shows the gel–sol transition temperatures (T_{gel}) of surfactant-**1** as a function of gelator concentration (mM) (A) and the van't Hoff relationship (B).³⁴ With increasing MGC, the T_{gel} values increase, and they gently increase above 18.3 mM of MGC, which indicates that the stability of the hydrogels is enhanced as the concentration increases. The T_{gel} values were 75 °C at 36.6 mM for DTMACI-1, 65 °C at 54.9 mM for HDTMACI-1, and 75 °C at 54.9 mM for DDMABr-1, and over these temperatures, they were not able to gel water even at 100 mM.

For all systems, linear relationships were observed in Fig. 5B. The gel–sol transition enthalpy (ΔH_{gel}) was determined from the slope of $\ln[1]$ versus $(T_{\text{gel}})^{-1}$ and listed in Table 2. The ΔH_{gel} was 52.6 kJ mol⁻¹ for the hydrogel based on DTMACI-1 and the largest value, while similar ΔH_{gel} values were observed for HDTMACI-1 and DDMABr-1 systems; 44.3 kJ mol⁻¹ and 43.3 kJ mol⁻¹. The MGC values are 3.7 mM for DTMACI-1 and 7.3 mM for HDTMACI-1 and DDMABr-1. In addition, the strength of the hydrogels follows the order: DTMACI-1 > HDTMACI-1 ≥ DDMABr-1. This behavior reflects the results of ΔH_{gel} . The ΔH_{gel} value of the hydrogel based on DTMACI-1, which forms a relatively rigid nanofiber, is large because the ΔH_{gel} corresponds to the energy of disassembly from the supramolecular polymer to the monomer in the gel–sol transition.



Scheme 2 Tentative illustration of hydrogelation mechanism.

Conclusions

We revealed the cationic surfactant-triggered formation of a L-valine derivative having a negative charge (**1**). Although this compound is water-soluble and has no hydrogelation properties, it forms a hydrogel in the presence of and during addition of a cationic surfactant below 18.3 mM. The FT-IR results indicate that the driving forces for the self-assembly of surfactant-**1** into nanofibers (hydrogelation) are hydrophobic and hydrogen bonding interactions. The fluorescence spectroscopy using ANS as a probe demonstrates that some aggregates, such as micelles, play an important role in the self-assembly of **1** into a nanofiber through an electrostatic interaction and the ANS molecules are incorporated into a hydrophobic field in the nanofibers of **1**.

Experimental

Materials and instrumentation

Compound **1** was prepared according to the literature.²⁵ All chemicals were of the highest commercially available grade and used without further purification. All solvents used in the syntheses were purified, dried, or freshly distilled as required.

The elemental analyses were performed using a Perkin-Elmer series II CHNS/O analyzer 2400. The FT-IR spectra were recorded on a JASCO FS-420 spectrometer. The transmission electron microscope (TEM) images were obtained using a JEOL JEM-2010 electron microscope at 200 kV. The field emission scanning electron microscope (FE-SEM) observations were carried out using a Hitachi S-5000 field emission scanning electron microscope. The ¹H-NMR spectra were measured using a Bruker AVANCE 400 spectrometer with

TMS in organic solvents and DSS in D₂O as the standard. The UV-Vis absorption spectra were acquired on a JASCO V-570 UV/VIS/NIR spectrometer. The emission spectra were recorded on a JASCO FP-750 spectrofluorometer.

Methods

Gelation test. The formation of a hydrogel was evaluated by a tube inversion method. For method 1, the final concentration of gelators is 18.3 mM.

Method 1. A mixture of a weighed gelator in an aqueous solution of surfactants (1 ml) in a sealed test tube was heated until a clear solution appeared, and then the sample was allowed to stand at 25 °C for 4 h.

Method 2. To an aqueous solution (1.8 ml) of gelators, an aqueous solution of surfactant (0.2 ml) was added in a vial (15 mm in diameter) with vigorous stirring, and then the capped vial was allowed to stand at 25 °C for 1 h.

Transmission electron microscope (TEM). Samples were prepared as follows: the aqueous solutions of the gelators were dropped on a collodion- and carbon coated 400 mesh copper grid and dried in a vacuum for 24 h. After negative staining by osmic acid overnight, the grids were dried under reduced pressure for 2 h.

Field emission scanning electron microscope (FE-SEM). Samples were prepared as follows: the xerogels were prepared from the organogels and hydrogels and dried in a vacuum for 24 h. The dried xerogels were shadowed to ca. 10 nm thick with Pt-Pd by sputtering.

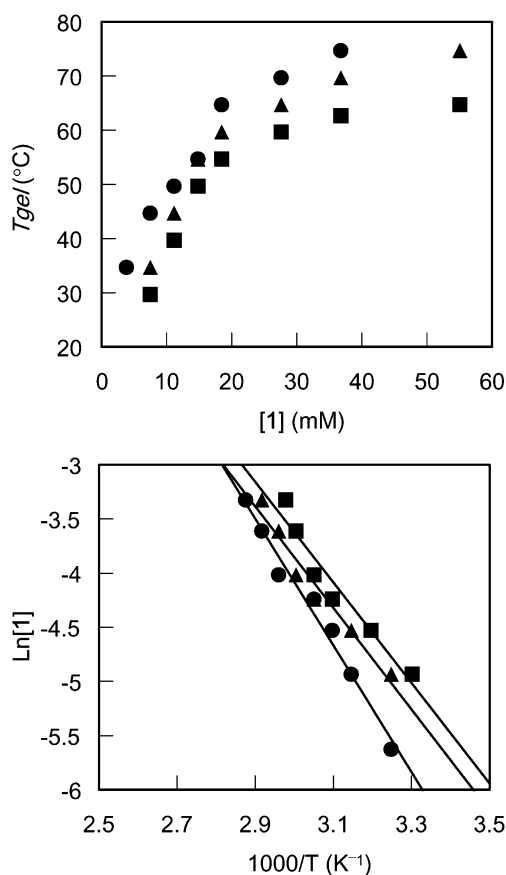


Fig. 5 Gel-sol transition temperatures (T_{gel}) of surfactant-1 (0.4 : 1) as a function of the gelator concentration (mM) (A) and the van't Hoff relationships (B). (●): DTMACI-1; (■): HDTMACI-1; (▲): DDMABr-1.

FT-IR study. FT-IR spectroscopy was performed in D_2O and chloroform operating at a 2 cm^{-1} resolution with 32 scans. The spectroscopic cell with a CaF_2 window and $25\text{ }\mu\text{m}$ spacers was used for the measurements.

Fluorescence study. Fluorescence spectra were measured at $[ANS] = 2.0 \times 10^{-5}\text{ M}$, $[I] = 18.3\text{ mM}$ (10 mg mL^{-1}) and $[DTMACI] = 7.28$ or 30.0 mM . Excitation is 356 nm .

Gel strength. The gel strength of the hydrogels was measured and evaluated as the power necessary to sink a cylinder bar (10 mm in diameter) 4 mm deep in the gels. Samples were prepared in a vial (15 mm in diameter).

Acknowledgements

This study is supported by a Grant-in-Aid for the 21st Century COE Program and a Grant-in-Aid for Exploratory Research

(No. 17655049) by the Ministry of Education, Culture, Sports, Science and Technology of Japan and by Tokuyama Science Foundation.

References

- 1 R. Langer, *Acc. Chem. Res.*, 2000, **33**, 94.
- 2 N. A. Peppas, Y. Huang, M. Tottes-Lugo, J. H. Ward and J. Zhang, *Annu. Rev. Biomed. Eng.*, 2000, **2**, 9.
- 3 K. Yong and D. J. Mooney, *Chem. Rev.*, 2001, **101**, 1869.
- 4 Low Molecular Mass Gelators: Design, Self-assembly, Function, *Top. Curr. Chem.*, ed. F. Fages, Springer, Berlin, 2005, **256**.
- 5 *Molecular Gels: Materials with Self-assembled Fibrillar Networks*, ed. P. Terech and R. G. Weiss, Springer, Dordrecht, 2006.
- 6 P. Terech and R. G. Weiss, *Chem. Rev.*, 1997, **97**, 3313.
- 7 J. H. van Esch and B. L. Feringa, *Angew. Chem., Int. Ed.*, 2000, **39**, 2263.
- 8 L. A. Estroff and A. D. Hamilton, *Chem. Rev.*, 2004, **104**, 1201.
- 9 M. de Loos, B. L. Feringa and J. H. van Esch, *Eur. J. Org. Chem.*, 2005, 3615.
- 10 N. M. Sangeetha and U. Maitra, *Chem. Soc. Rev.*, 2005, **34**, 821.
- 11 F. Lequeux and S. J. Candau, *ACS Symp. Ser.*, 1994, **578**, 51.
- 12 A. Heeres, C. van der Pol, M. Stuart, A. Friggeri, B. L. Feringa and J. van Esch, *J. Am. Chem. Soc.*, 2003, **125**, 14252.
- 13 B. L. Feringa, R. A. van Delden, N. Koumura and E. M. Geertsema, *Chem. Rev.*, 2000, **100**, 1789.
- 14 H. Koshima, W. Matsusaka and H. Yu, *J. Photochem. Photobiol., A*, 2003, **156**, 83.
- 15 J. J. D. de Jong, L. N. Lucas, B. M. Kellogg, J. H. van Esch and B. L. Feringa, *Science*, 2004, **304**, 278.
- 16 S. Yagai, T. Nakajima, K. Kishikawa, S. Kohmoto, T. Karatsu and A. Kitamura, *J. Am. Chem. Soc.*, 2005, **127**, 11134.
- 17 A. R. Hirst and D. K. Smith, *Chem.-Eur. J.*, 2005, **11**, 5496.
- 18 J. J. D. de Jong, T. Naota and H. Koori, *J. Am. Chem. Soc.*, 2005, **127**, 9324.
- 19 T. D. Tiemersma-Wegman, J. H. van Esch and B. L. Feringa, *J. Am. Chem. Soc.*, 2005, **127**, 13804.
- 20 C. Wang, D. Zhang and D. Zhu, *J. Am. Chem. Soc.*, 2005, **127**, 16372.
- 21 S. Wang, W. Shen, Y. Feng and H. Tian, *Chem. Commun.*, 2006, 1497.
- 22 S. Miljanić, L. Frkanec, Z. Meić and M. Žinic, *Eur. J. Org. Chem.*, 2006, 1323.
- 23 J. B. Beck and S. J. Rowan, *J. Am. Chem. Soc.*, 2003, **125**, 13922.
- 24 M. Numata, K. Sugiyasu, T. Hasegawa and S. Shinkai, *Angew. Chem., Int. Ed.*, 2004, **43**, 3279.
- 25 M. Suzuki, T. Sato, H. Shirai and K. Hanabusa, *New J. Chem.*, 2006, **30**, 1184.
- 26 *Surfactants and Interfacial Phenomena*, ed. M. J. Rosen, John Wiley and Sons, New York, 2nd edn., 1989.
- 27 K. Hanabusa, T. Miki, Y. Taguchi, T. Koyama and H. Shirai, *J. Chem. Soc., Chem. Commun.*, 1993, 1382.
- 28 A. R. Hirst and D. K. Smith, *Chem.-Eur. J.*, 2005, **11**, 5496.
- 29 M. Suzuki, M. Yumoto, M. Kimura, H. Shirai and K. Hanabusa, *Chem.-Eur. J.*, 2003, **9**, 348.
- 30 M. Suzuki, S. Owa, M. Kimura, A. Kurose, H. Shirai and K. Hanabusa, *Tetrahedron Lett.*, 2005, **46**, 303.
- 31 L. Stryer, *Science*, 1968, **162**, 526.
- 32 R. P. DeToma, J. H. Easter and L. Brand, *J. Am. Chem. Soc.*, 1976, **98**, 5001.
- 33 M. Suzuki, M. Yumoto, M. Kimura, H. Shirai and K. Hanabusa, *Tetrahedron Lett.*, 2004, **45**, 2947.
- 34 S. H. Seo and J. Y. Chang, *Chem. Mater.*, 2005, **17**, 3249.